Note

Anti-MUC1 Aptamer/Negatively Charged Amino Acid Dendrimer Conjugates for Targeted Delivery to Human Lung Adenocarcinoma A549 Cells

Marie Masuda,[a] Shigeru Kawakami,*[,b] Wassana Wijagkanalan,[a] Tadaharu Suga,[b] Yuki Fuchigami,[b] Fumiyoshi Yamashita,[a] and Mitsuru Hashida[a,c]

[a] *Department of Drug Delivery Research, Graduate School of Pharmaceutical Sciences, Kyoto University; 46–29 Yoshida-shimoadachi-cho, Sakyo-ku, Kyoto 606–8501, Japan:* [b] *Department of Pharmaceutical Informatics, Graduate School of Biomedical Sciences, Nagasaki University; 1–7–1 Sakamoto-machi, Nagasaki 852–8588, Japan: and* [c] *Institute for Integrated Cell-Material Sciences (iCeMS), Kyoto University; Yoshida-ushinomiya-cho, Sakyo-ku, Kyoto 606–8302, Japan.*

Received June 24, 2016; accepted July 11, 2016

We previously developed a negatively charged amino acid dendrimer to address the safety concerns associated with the constituent unit of these systems, which resulted in the formation of a sixth-generation glutamic acid-modified dendritic poly(L-lysine) system (KG6E). The aim of this study was to develop a nanocarrier for targeted drug delivery into cancer cells. In this study, we have synthesized a conjugate material consisting of anti-mucin 1 (MUC1) aptamer (anti-MUC1 apt) and KG6E (anti-MUC1 apt/KG6E) for targeted drug delivery to human lung adenocarcinoma A549 cells, which express high levels of the MUC1. The anti-MUC1 apt/KG6E was efficiently internalized by the A549 cells and subsequently transported to the endosomal and lysosomal compartments. In contrast, the cellular association of the sequence scrambled aptamer/KG6E conjugate (scrambled apt/KG6E) was much lower than that of the anti-MUC1 apt/KG6E in A549 cells. These results suggest that our newly developed anti-MUC1 apt/KG6E can be internalized in A549 cells *via* a MUC1 recognition pathway.

Key words drug delivery; targeting; aptamer; dendrimer; mucin 1 (MUC1)

Aptamers (apts) are a class of single-stranded nucleic acid ligands that are capable of binding to an individual target molecule with high affinity and specificity.[1)] Notably, aptamers are less immunogenic than antibodies, making them better suited for systemic administration and long term therapy.[2)] Recently, an DNA aptamer derived from 5TR1 was discovered for high binding affinity to mucin 1 (MUC1), which is a large cellular surface mucin glycoprotein involved in cell proliferation, differentiation, apoptosis and secretion of specialized cellular prodicts.[3,4)] Some of the glycoforms of membrane-associated MUC1 represent an important class of tumor surface markers that are uniquely and abundantly expressed on a broad range of epithelial cancer cells. Furthermore, MUC1 is rapidly recycled through several intracellular compartments. Several recent studies have reported the application of anti-MUC1 apt as a ligand for nanoparticles to specifically target various epithelial cancer cells.[5–7)]

Dendrimers are highly compact nanostructures composed of numerous branched layers and have consequently been studied in great detail as potential carriers for the development of drug delivery systems.[8)] Good safety and target cell-specificity are important properties for the successful development of drug delivery systems based on dendrimers. Niidome and colleagues successfully developed a sixth-generation dendritic poly(L-lysine) system (KG6).[9)] We previously developed an amino acid dendrimer with the aim of addressing the safety issues associated with the constituent unit, which resulted in glutamic acid-modified KG6 (KG6E).[10)] Notably, KG6E was negatively charged and showed very little cytotoxicity compared with the positively charged KG6 or polyamidoamine (PAMAM) dendrimer in cultured cells. In addition, we found that KG6E-trastuzumab conjugates can be internalized by HER2-positive human breast cancer cells *via* trastuzumab recognition. Based on our knowledge, we envisaged that conjugates composed of an anti-MUC1 apt and KG6E (anti-MUC1 apt/KG6E) would be efficient nanocarrier systems for targeting epithelial cancer cells. However, very little is currently known about the suitability of this conjugate as a nanocarrier for targeted therapy.

In this study, we have synthesized the anti-MUC1 apt/KG6E and evaluated its cellular uptake properties using human lung adenocarcinoma A549 cells, which express high levels of the MUC1.[11)]

MATERIALS AND METHODS

Materials DNA oligomers labeled with Alexa Fluor® 488 were obtained from Nihon Bio Service (Asaka, Japan), whereas those modified with a 5′-thiol moiety were obtained from Hokkaido System Science Co., Ltd. (Hokkaido, Japan). Succinimidyl-4-(*N*-maleimidomethyl)cyclohexane-1-carboxy-(6-amidocaproate) (LC-SMCC) was purchased from Pierce (Rockford, IL, U.S.A.). Alexa Fluor® 488 succinimidyl esters, transferrin, Alexa Fluor® 568 conjugate, LysoTracker®Red DND-99 and Anti-Alexa Fluor® 488, Rabbit immunoglobulin (Ig)G Fraction were purchased from Molecular Probes (Eugene, OR, U.S.A.). All of the fluorescence labeling and modification experiments involving on the oligonucleotides were conducted during the custom synthesis process. The sequences of the anti-MUC1 and sequence-scrambled aptamers were 5′-AAT GAC AGA ACA CAA CAT T-3′ and 5′-GAT CGA TCG ATC GAT CGA T-3′, respectively.

* To whom correspondence should be addressed. e-mail: skawakam@nagsaki-u.ac.jp

Cell Lines and Buffers A549 cells were purchased from American Type Cell Collection (ATCC; Manassas, VA, U.S.A.) and grown in a humidified atmosphere containing in 5% CO_2 at 37°C with RPMI1640 medium (Nissui Pharmaceutical Co., Ltd., Tokyo, Japan) supplemented with 10% fetal bovine serum (FBS), 100 U/mL penicillin, 100 μg/mL streptomycin and L-glutamine.

Synthesis of the Apt/KG6E Conjugates KG6 and KG6E were synthesized according to a previously reported method.[3,8] Alexa Fluor® 488-labeled KG6E (KG6E-AF) was synthesized and purified by gel filtration chromatography. Then, KG6E-AF (26 mg, 0.80 μmol) was subsequently treated with LC-SMCC (10 mg, 8.0 μmol) in *N*,*N*-dimethylformamide at room temperature for 16 h to allow for the introduction of a maleimide group. Upon completion of the reaction, the excess reagent was removed by gel filtration. The resulting maleimide-linked KG6E-AF material was immediately reacted with 5′-thiol-modified aptamer (10 mg, 0.80 μmol) in Dulbecco's phosphate-buffered saline (DPBS)-ethylenediaminetetraacetic acid (EDTA) buffer at room temperature, before being concentrated on a VIVASPIN 20 column (MWCO 3000) and purified by 6% polyacrylamide gel electrophoresis containing 7 M urea.

Physicochemical Properties The mean sizes of KG6E and the apt/KG6E conjugates were measured using a Zetasizer Nano ZS system (Malvern Instruments Ltd., Worcester, U.K.). All of these measurements were conducted in triplicate.

Flow Cytometry Analysis After an incubation period of 48 h, the A549 cells (5×10^4 cells) were incubated with the aptamer, KG6E-AF, a sequence scrambled apt/KG6E conjugate (scrambled apt/KG6E) or anti-MUC1 apt/KG6E in DPBS containing 5 mM $MgCl_2$ and 0.9 mM $CaCl_2$ at 37°C for 1 h. The cells were suspended in fluorescent activated cell sorter (FACS) buffer, and their fluorescence intensities were measured by flow cytometry. Flow cytometry analysis was performed on a FACScan system (Becton Dickinson Immunocytometry Systems, San Jose, CA, U.S.A.).

Confocal Microscopy A549 cells were used for each experiment after incubation for 48 h. For the internalization experiment, A549 cells (1.25×10^4 cells) were incubated with anti-MUC1 apt/KG6E in DPBS containing 5 mM $MgCl_2$ and 0.9 mM $CaCl_2$ at 37°C for 1 h. For the co-localization experiment, A549 cells (1.25×10^4 cells) were incubated with transferrin Alexa Fluor® 568 conjugated (50 μg/mL) or LysoTrackerRed DND-99 (75 μM) at 37°C for 1 h in growth medium without FBS. The cells were then incubated with anti-MUC1 apt/KG6E in DPBS containing 5 mM $MgCl_2$ and 0.9 mM $CaCl_2$ at 37°C for 3 h, before being fixed with 4% paraformaldehyde solution and analyzed with a C1-si confocal laser scanning microscope (Nikon, Tokyo, Japan).

Calculation of the Dissociation Constant (K_d) for the Ligand of the Anti-MUC1 apt/KG6E to the A549 Cells After an incubation period of 48 h, the A549 cells (5×10^4 cells) were incubated with anti-MUC1 apt/KG6E at several different concentrations in the range of 0.1 to 400 nM in DPBS containing 5 mM $MgCl_2$ and 0.9 mM $CaCl_2$ at 37°C for 30 min. The mean fluorescence intensity of the anti-MUC1 apt/KG6E bound to the A549 cells were measured by flow cytometry analyses as previously noticed. The K_d value was determined as the concentration of anti-MUC1 apt/KG6E required to achieve 50% of the maximum fluorescence intensity.

Statistical Analysis The statistical difference was determined by unpaired Student's *t*-test. Difference with $p<0.05$ was considered significant.

RESULTS

Synthesis and Characterization The full-length aptamer selected from the library of Ferreira *et al.*[4] are 70-mer sequences. It is noteworthy that the efficient binding of an aptamer to its target does not always require the full-length sequence of the nucleotides. Therefore, the original sequence of this aptamer was further shortened based on its predicted secondary structure[12] and the results of a binding assay con-

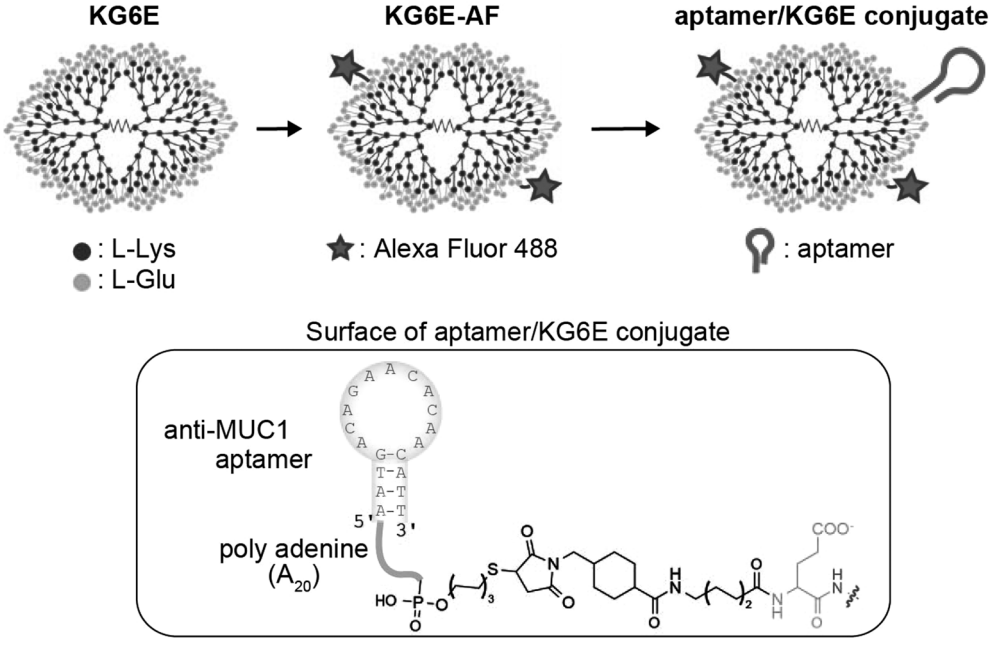

Fig. 1. Scheme for the Synthesis of the Anti-MUC1 Apt/KG6E

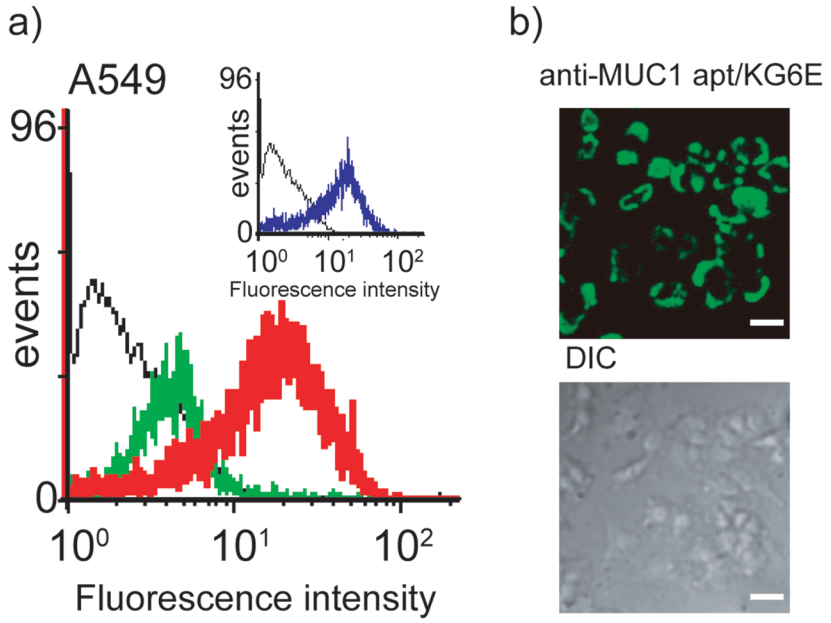

Fig. 2. Cellular Association with the A549 Cells

(a) Selective binding of the anti-MUC1 aptamer and anti-MUC1 apt/KG6E to the MUC1 determinants in A549 cells. The A549 cells were stained with Alexa Fluor® 488-labeled anti-MUC1 aptamer (blue), anti-MUC1 apt/KG6E (red) and intact KG6E (green) for 1 h, before being analyzed by flow cytometry. (b) Cellular association of the Alexa Fluor® 488-labeled anti-MUC1 apt/KG6E, as monitored by confocal microscopy. The confocal microscopy images were recorded after 1 h of incubation. Scale bar: 30 μm. The evaluated concentration of anti-MUC1 apt/KG6E was 1, 10, 50, 100, and 200 nM.

ducted by flow cytometry. The results of this optimization process revealed that a 19-mer sequence showed the highest binding affinity of all of the sequences tested towards A549 cells (Fig. 1). The structure of the synthesized KG6E material was confirmed by matrix-assisted laser desorption/ionization time-of-flight mass spectrometry, which gave an *m/z* of 32,741.82 (calcd for $[M+H]^+$=32776.15). KG6E was fluorescently labeled using Alexa Fluor® 488, and an average of eight maleimide groups to react with 5′-thiol modified aptamer were introduced per molecule of KG6E-AF. For the conjugation of the aptamer to KG6E, we added an extra 20 adenine (A) bases to the 5′-terminal to ensure that the binding domains of the anti-MUC1 apt projected away from the surface of KG6E-AF, because they could otherwise interfere with the binding of the aptamer to the target. The conjugation of the aptamer to KG6E-AF was confirmed by polyacrylamide gel electrophoresis. There were several bands of conjugates that are comprised of one dendrimer and multiple aptamer. The physicochemical properties of KG6E and anti-MUC1 apt/KG6E were analyzed using a variety of different techniques. The mean diameters of anti-MUC1 apt/KG6E (10.5±0.058 nm), 2 molecules of anti-MUC1 aptamer conjugated with 1 molecule of KG6E (2-anti-MUC1 apt/KG6E) (13.6±0.100 nm) and 3 molecules of anti-MUC1 aptamer conjugated with 1 molecule of KG6E (3-anti-MUC1 apt/KG6E) (15.7±0.115 nm) conjugates were larger than that of the intact KG6E material (5.67±0.110 nm), which increased depending on the aptamer conjugation ratio.

Specific Binding to A549 Cells Apt-dependent binding was evaluated by flow cytometry based on a binding assay involving the anti-MUC1 apt/KG6E. The results revealed that the anti-MUC1 apt/KG6E had a high affinity for A549 cells (Fig. 2a). Given that the anti-MUC1 apt/KG6E, 2-anti-MUC1/KG6E and 3-anti-MUC1/KG6E exhibited similar levels of cellular association, the anti-MUC1 apt/KG6E was selected for further experiments. Furthermore, the confocal microscopy images shown in Fig. 2b demonstrated the presence of very bright fluorescence (green) on the periphery of the A549 cells after they had been incubated for 1 h with the anti-MUC1 apt/KG6E. The binding properties of the scrambled apt/KG6E were also measured for comparison. As shown in Fig. 3, the cellular association of the anti-MUC1 apt/KG6E was much higher than that of the scrambled apt/KG6E in A549 cells at every concentration tested (the K_d value of the anti-MUC1 apt/KG6E was 62.2 nM).

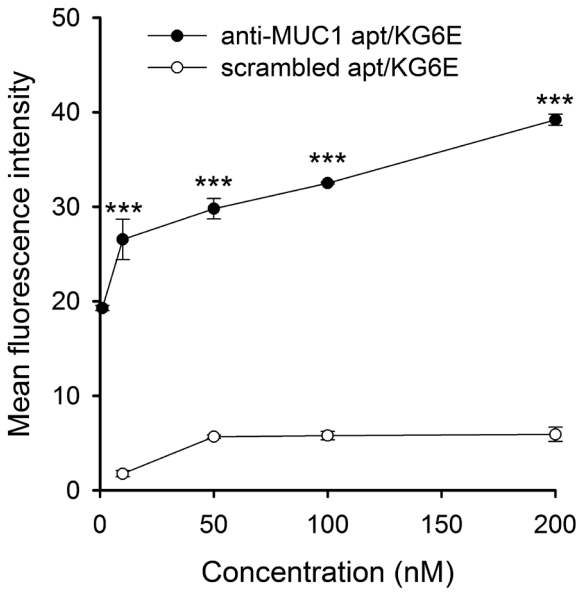

Fig. 3. Concentration-Dependent Association with A549 Cells

The treated A549 cells were analyzed by flow cytometry over 10000 events. Incubations were performed at 37°C for 1 h. All of these data points represent the average relative mean fluorescence intensities from three independent experiments. Unpaired Student's *t*-test was performed to determine the significance (***$p<0.001$).

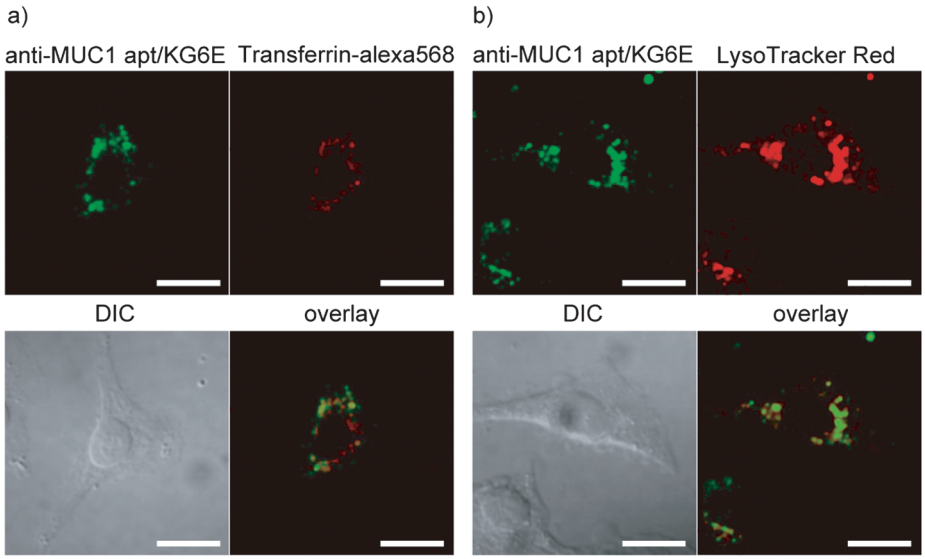

Fig. 4. Intracellular Distribution of the Anti-MUC1 apt/KG6E and the Different Markers for the Organelles in the A549 Cells

(a) Transferrin or (b) LysoTracker in the lysosomes. From left to right (top): Images for the anti-MUC1 apt/KG6E, transferrin or LysoTracker, (bottom) bright field channel and overlay of the fluorescence channels, respectively. Scale bar: 20 μm.

Intracellular Localization in A549 Cells To determine whether anti-MUC1 apt/KG6E was internalized into A549 cells, we evaluated the localization of this conjugate in A549 cells by confocal microscopy after incubation for 3 h. As shown in Fig. 4, the anti-MUC1 apt/KG6E was transported into the endosomal and lysosomal compartments.

DISCUSSION

We envisaged that the anti-MUC1 apt/KG6E would be useful as a carrier for drug delivery in the cells. Therefore, we evaluated the cellular association and internalization of the anti-MUC1 apt/KG6E using A549 cells. As shown in Figs. 2 to 4, the anti-MUC1 aptamer and anti-MUC1 apt/KG6E directed at MUC1 were rapidly bound to the MUC1 and internalized by the A549 cells, where they were localized in endosomes and lysosomes. Notably, the cellular association of the scrambled apt/KG6E in A549 was significantly lower than that of the anti-MUC1 apt/KG6E, suggesting the sequence-dependent specific recognition of MUC1 by the anti-MUC1 apt/KG6E (Fig. 3). In addition, the anti-MUC1 apt/KG6E was localized in the endosomes and lysosomes of the A549 cells (Fig. 4). These results therefore suggest that the association and internalization of the anti-MUC1 apt/KG6E occur *via* MUC1 recognition in A549 cells.

Nanocarriers need to display high levels of safety and biocompatibility to be used in drug delivery applications. Cationic polymers generally exhibit high cellular toxicity *via* the formation of electrostatic interactions with the negatively charged surfaces of the cells.[8] With this in mind, the anti-MUC1 aptamer was conjugated with the negatively changed KG6E in the current study for safety.

In summary, we developed the anti-MUC1 apt/KG6E for the selective targeting of A549 cells. The new anti-MUC1 apt/KG6E was efficiently internalized and subsequently transported to the endosomal and lysosomal compartments in A549 cells. These results therefore suggest that the anti-MUC1 apt/KG6E is readily recognized by MUC1 and sorted to lysosomes. The result of this study will provide valuable information for the development of aptamer-conjugated amino acid dendrimers for use in targeted drug delivery systems.

Acknowledgment The authors would like to thank Professor Takuro Niidome, Kumamoto University, Japan, for completing the synthesis of KG6E.

Conflict of Interest The authors declare no conflict of interest.

REFERENCES AND NOTES

1) Rimmele M. Nucleic acid aptamers as tools and drugs: recent developments. *ChemBioChem*, **4**, 963–971 (2003).
2) Vorhies JS, Nemunaitis JJ. Nucleic acid aptamers for targeting of shRNA-based cancer therapeutics. *Biologics*, **1**, 367–376 (2007).
3) Hollingsworth MA, Swanson BJ. Mucins in cancer: protection and control of the cell surface. *Nat. Rev. Cancer*, **4**, 45–60 (2004).
4) Ferreira CS, Cheung MC, Missailidis S, Bisland S, Gariépy J. Phototoxic aptamers selectively enter and kill epithelial cancer cells. *Nucleic Acids Res.*, **37**, 866–876 (2009).
5) Kurosaki T, Higuchi N, Kawakami S, Higuchi Y, Nakamura T, Kitahara T, Hashida M, Sasaki H. Self-assemble gene delivery system for molecular targeting using nucleic acid aptamer. *Gene*, **491**, 205–209 (2012).
6) Sayari E, Dinarvand M, Amini M, Azhdarzadeh M, Mollarazi E, Ghasemi Z, Atyabi F. MUC1 aptamer conjugated to chitosan nanoparticles, an efficient targeted carrier designed for anticancer SN38 delivery. *Int. J. Pharm.*, **473**, 304–315 (2014).
7) Ghasemi Z, Dinarvand R, Mottaghitalab F, Esfandyari-Manesh M, Sayari E, Atyabi F. Aptamer decorated hyaluronan/chitosan nanoparticles for targeted delivery of 5-fluorouracil to MUC1 overexpressing adenocarcinomas. *Carbohydr. Polym.*, **121**, 190–198 (2015).
8) Wijagkanalan W, Kawakami S, Hashida M. Designing dendrimers for drug delivery and imaging: pharmacokinetic considerations. *Pharm. Res.*, **28**, 1500–1519 (2011).
9) Ohsaki M, Okuda T, Wada A, Hirayama T, Niidome T, Aoyagi H. *In vitro* gene transfection using dendritic poly(L-lysine). *Bioconjug.*

Chem., **13**, 510–517 (2002).
10) Miyano T, Wijagkanalan W, Kawakami S, Yamashita F, Hashida M. Anionic amino acid dendrimer-trastuzumab conjugates for specific internalization in HER2-positive cancer cells. *Mol. Pharm.*, **2**, 30–37 (2010).
11) Zhang K, Wang J, Jiang H, Xu X, Wang S, Zhang C, Li Z, Gong X, Lu W. Tanshinone IIA inhibits lipopolysaccharide-induced MUC1 overexpression in alveolar epithelial cells. *Am. J. Physiol. Cell Physiol.*, **306**, C59–C65 (2014).
12) Predictions of RNA secondary structures and folding free energies were carried out by an RNAstructure Version 4.4 program (Mathews DH, Zuker M, Turner DH).